Session I

Nuclear data needs and impact

Chair: Urszula Woznicka

Impact of nuclear data uncertainties on neutronics parameters of MYRRHA/XT-ADS

Takanori Sugawara[1,2], Alexey Stankovskiy[1], Massimo Sarotto[1,3], Gert Van den Eynde[1]
[1]SCK·CEN, Mol, Belgium
[2]JAEA, Ibaraki, Japan
[3]ENEA, Bologna, Italy

Abstract

A flexible fast spectrum research reactor MYRRHA able to operate in subcritical (driven by a proton accelerator) and critical modes is being developed in SCK·CEN. In the framework of IP EUROTRANS programme the XT-ADS model has been investigated for MYRRHA. In this study, the sensitivity and uncertainty analysis was performed to comprehend the reliability of the XT-ADS neutronics design. The calculated sensitivity coefficients for neutronics parameters varied significantly between calculation models. The uncertainties deduced from the covariance data strongly depend on the original covariance data. The calculated nuclear data uncertainties could not meet the target accuracy. To improve uncertainties, the integral experiments in adequate conditions are expedient.

Introduction

SCK·CEN, the Belgian Nuclear Research Centre in Mol is designing a Multi-purpose Hybrid Research Reactor for High-tech Applications (MYRRHA) [1]. The Accelerator-Driven System (ADS) concept has been chosen as a basis for this reactor, assuming that it can operate in both sub-critical and critical modes. The design studies for eXperimental demonstration of technical feasibility of Transmutation in an Accelerator-Driven System (XT-ADS) have been conducted in the framework of IP EUROTRANS FP6 project [2].

Recently, the sensitivity and uncertainty (S/U) analysis has been reported aiming to identify target nuclear data accuracies for nuclear systems modelling [3,4], the influence of covariance data on the criticality safety was assessed in [5] and the evaluation of the effect of hypothetical MA-loaded critical experiments on a reduction of the data uncertainty has been performed in [6]. Since uncertainties are calculated by the sensitivity coefficients and covariance data from nuclear data libraries, the reliability of the results in the S/U analysis is based on these two parameters. It has been pointed out [7] that the covariance data contained in JENDL-3.3 [8] may underestimate the uncertainty in the nuclear design of the transmutation systems. It was also mentioned that further discussion on the application of the S/U analysis to the nuclear design is required.

This paper reports the comparison of the sensitivity coefficients calculated for different calculation models and the uncertainties deduced from various covariance data for the discussion on the reliability of XT-ADS neutronics design. Sensitivity analysis is based on the comparison of three-dimensional heterogeneous and two-dimensional RZ calculation models. Three covariance data sets were employed to perform uncertainty analysis. Besides that, the uncertainties were compared with the results calculated by the MCNPX code [9] to discuss the uncertainty reliability.

Methods

XT-ADS

SCK·CEN has been working since 1998 on the design of MYRRHA in order to replace the aging BR2 (Belgian Reactor 2) multi-functional materials testing reactor which operates since 1962. The ADS concept has been chosen as a basis for this reactor, assuming that it can operate in both sub-critical and critical modes. In the framework of PDS-XADS (Preliminary Design Study of an eXperimental ADS) FP5 project, the basic design of installation has been elaborated [1]. The proton accelerator is coupled with multiplying core loaded with MOX fuel cooled by liquid lead-bismuth eutectic (LBE) which serves also as spallation target. The design studies have been continued in the framework of IP EUROTRANS FP6 project. The goal of the project was to develop an advanced design leading to the XT-ADS. The XT-ADS was intended to be a test bench for the main components and irradiation scheme of a full-scale ADS, EFIT (European Facility for an Industrial Transmutation) [10].

Three-dimensional heterogeneous and two-dimensional RZ homogenized models

The XT-ADS is a LBE cooled pool-type 100 MWth subcritical reactor with MOX fuel containing 35 wt.% Pu [11]. The core is driven by the proton accelerator (proton energy 600 MeV, maximum current 2.5 mA). The layout of the XT-ADS core is illustrated in Figure 1, a. Three central assemblies serve as feeders for liquid lead-bismuth spallation target. The core itself contains 72 fuel assemblies and 8 assemblies are used as In-Pile-Section (IPS) dedicated for the irradiation and measurements. There are also dummy assemblies filled with LBE but designed to host control rods and mock-up reflecting stainless steel assemblies on the periphery of the core.

To estimate the difference in the sensitivity coefficients between calculation models, a two-dimensional RZ calculation model for the XT-ADS was also employed. A conceptual diagram of the RZ calculation model is shown in Figure 1, b. Each region was homogenized. SS50 denotes the core support region which was homogenized as fifty-fifty volume ratio of LBE and T91.

Figure 1: a) Three-dimensional heterogeneous calculation model for XT-ADS
b) Two-dimensional RZ homogenized calculation model for XT-ADS

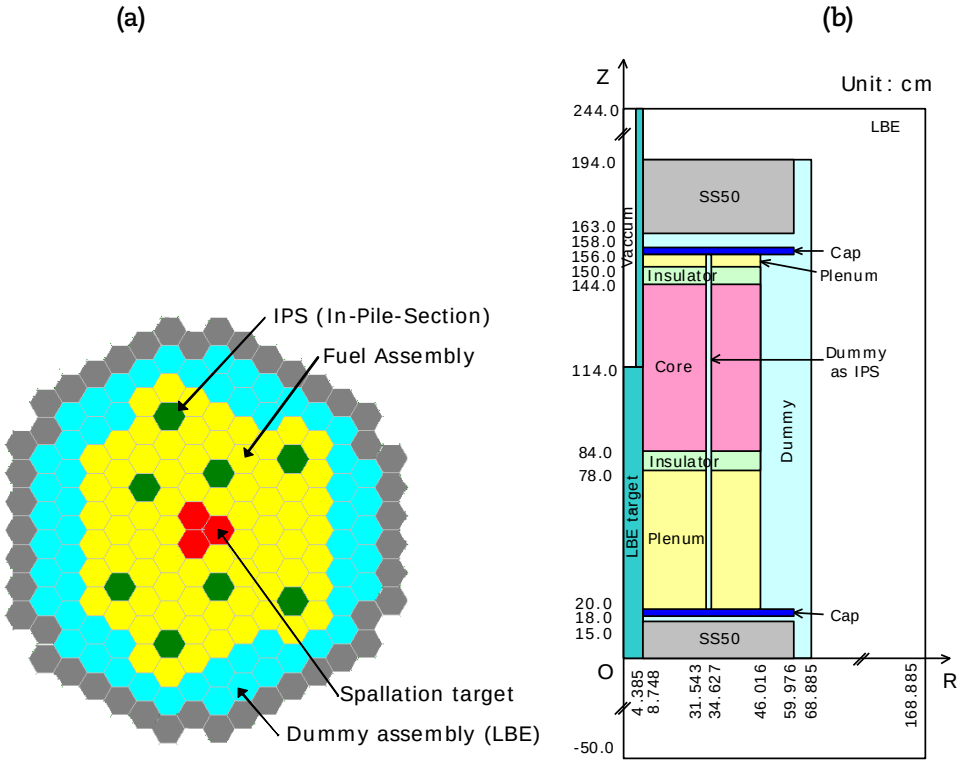

Sensitivity coefficients and uncertainties deduced from covariance data

Generally, the sensitivity coefficient S of a parameter R against parameter Σ is defined as

$$S = \frac{dR}{R} \Big/ \frac{d\Sigma}{\Sigma} \tag{1}$$

Effective neutron multiplication factor k_{eff} plays role of R and microscopic cross-section data for each particular neutron induced reaction are supposed as Σ. Applying the perturbation theory to the Boltzmann transport equation, one can obtain [12]

$$S = \frac{\partial k}{k} \Big/ \frac{\partial \Sigma(r)}{\Sigma(r)} = -k\Sigma(r) \frac{\left\langle \phi^{+}(\xi) \left(\frac{\partial A[\Sigma(\xi)]}{\partial \Sigma(r)} - \frac{1}{k} \frac{\partial B[\Sigma(\xi)]}{\partial \Sigma(r)} \right) \phi(\xi) \right\rangle}{\langle \phi^{+}(\xi) B[\Sigma(\xi)] \phi(\xi) \rangle} \tag{2}$$

Here ξ is the phase space vector, ϕ^{+} is adjoint neutron flux, A is an operator of the left-hand side of the transport equation except fission term and B is an operator for the fission term of transport equation.

The variance for the k_{eff} is determined as [7,12]

$$\sigma^2_{k^{i,j}_{x,y}} = G_{\alpha^i_x} M_{\alpha^i_x \alpha^j_y} G^t_{\alpha^j_y}, \tag{3}$$

where $k^{i,j}_{x,y}$ is 2D-dependence of k_{eff} from x, y (reaction type) and i,j (nuclide type); $G_{\alpha^i_x}$ and $G^t_{\alpha^j_y}$ are group-wise sensitivity vectors (the latter is transposed one) of length G (G is the number of energy groups), α is the parameter (cross-section) with respect to which the k_{eff} sensitivity is calculated; $M_{\alpha^i_x \alpha^j_y}$ is $G \times G$ size covariance matrix.

Calculation tool

The SCALE-6 (Standardized Computer Analyses for Licensing Evaluation) [13] code was employed for the S/U analysis. It consists of many calculation modules and utilities for calculations of reactor physics, criticality safety and radiation shielding. For the S/U analysis, the TSUNAMI-3D module was employed. This module performs the calculation of the sensitivity coefficients for the effective neutron multiplication factor by using the forward and adjoint fluxes data. After the sensitivity analysis, this module calculates the uncertainty deduced from the covariance data contained in the nuclear data library. For the neutron transport calculation, the KENO-VI multigroup Monte Carlo transport module was used with a detailed three-dimensional calculation model. In this calculation, the 238 group nuclear data library based on ENDF/B-VII.0 data [14] was employed. For the uncertainty analysis, 44 energy groups, which is a default structure in the TSUNAMI-3D module, was used.

Results

Sensitivity coefficients

The sensitivity analysis with respect to models was performed to reflect the differences in their nature. The RZ calculation model was prepared aiming to match basic integral neutronics parameters calculated with full 3D model taking into account that clear differences will exist between these calculation models. The k_{eff} values calculated for both models reveal ~2000 pcm difference: for 3D heterogeneous model KENO-VI returns k_{eff} = 0.98305±0.00031 while RZ model gives k_{eff} = 0.96234±0.00032. The neutron spectrum in 3D model is harder than in RZ homogenized model [11] thus k_{eff} is higher.

Table 1 and Table 2 show the sensitivity coefficients calculated by the SCALE code with the 3D heterogeneous and RZ homogenized calculation models, respectively. Uranium and Plutonium isotopes, isotopes of LBE (Pb and Bi-209), as well as Fe-56 and O-16 were treated as main objects in the S/U analysis since their sensitivity coefficients dominate among the sensitivity coefficients for the keff of the XT-ADS core. The tables indicate that the total sensitivity of the neutron capture reaction in the RZ model is smaller than that in the 3D heterogeneous model, and coefficients for U-238 and Pu-239 are low enough. On the other hand, the sensitivity coefficients of the neutron induced fission reaction and average neutron release per fission event $\overline{\nu}$ in the 3D heterogeneous calculation model are higher than corresponding coefficients in the RZ model, especially for U-238 and Pu-240. This is also caused by the difference in the neutron spectra.

Table 1: Sensitivity coefficients calculated by SCALE-6 for 3D model

Nuclide	Capture	Fission	$\overline{\nu}$	Elastic	Inelastic	(n,2n)	Total
O-16	-1.23E-03			1.66E-02	-1.31E-04	-2.37E-10	1.53E-02
Fe-56	-1.97E-02			-6.71E-03	-4.92E-03	3.39E-06	-3.13E-02
Pb-204	-2.23E-03			5.17E-04	-9.79E-05	1.63E-06	-1.81E-03
Pb-206	-3.82E-03			3.05E-03	-1.57E-03	3.92E-05	-2.31E-03
Pb-207	-2.82E-03			2.14E-03	-1.32E-03	8.35E-05	-1.92E-03
Pb-208	-5.39E-04			4.53E-03	-8.81E-04	1.19E-04	3.23E-03
Bi-209	-8.82E-03			1.50E-02	-4.08E-03	3.17E-04	2.42E-03
U-235	-1.67E-03	8.60E-03	1.43E-02	1.28E-06	-3.43E-05	2.82E-06	2.12E-02
U-238	-1.02E-01	3.46E-02	5.53E-02	7.01E-05	-7.41E-03	4.79E-04	-1.90E-02
Pu-238	-3.70E-03	1.35E-02	1.99E-02	3.98E-06	-3.59E-05	1.60E-06	2.97E-02
Pu-239	-5.98E-02	4.71E-01	7.06E-01	-4.66E-04	-7.66E-04	3.48E-05	1.12E+00
Pu-240	-2.71E-02	5.68E-02	8.38E-02	1.11E-03	-5.74E-04	1.01E-05	1.14E-01
Pu-241	-6.06E-03	6.89E-02	1.04E-01	-3.86E-06	-7.96E-05	2.33E-05	1.67E-01
Pu-242	-6.79E-03	1.17E-02	1.72E-02	1.02E-04	-1.96E-04	7.90E-06	2.20E-02
Total	-2.46E-01	6.65E-01	1.00E+00	3.59E-02	-2.21E-02	1.12E-03	1.43E+00

Table 2: Sensitivity coefficients calculated by SCALE-6 for RZ model

Nuclide	Capture	Fission	$\overline{\nu}$	Elastic	Inelastic	(n,2n)	Total
O-16	-7.06E-04			3.34E-03	-7.42E-05	-3.44E-11	2.56E-03
Fe-56	-2.25E-02			4.01E-03	-1.74E-03	3.74E-06	-2.02E-02
Pb-204	-1.66E-03			2.24E-04	-4.10E-05	1.47E-06	-1.48E-03
Pb-206	-2.20E-03			8.45E-04	-6.25E-04	3.45E-05	-1.95E-03
Pb-207	-2.27E-03			6.41E-04	-3.87E-04	6.88E-05	-1.95E-03
Pb-208	-1.91E-04			1.06E-03	-5.65E-04	1.10E-04	4.14E-04
Bi-209	-6.66E-03			5.15E-03	-2.08E-03	2.67E-04	-3.32E-03
U-235	-2.99E-03	1.14E-02	1.91E-02	-1.60E-06	-1.65E-05	1.77E-06	2.75E-02
U-238	-1.73E-01	1.55E-02	2.41E-02	3.23E-04	-2.70E-03	3.20E-04	-1.35E-01
Pu-238	-6.70E-03	1.07E-02	1.58E-02	-4.80E-06	-1.40E-05	1.05E-06	1.98E-02
Pu-239	-1.34E-01	5.00E-01	7.62E-01	-8.46E-04	-2.96E-04	2.19E-05	1.13E+00
Pu-240	-5.27E-02	2.36E-02	3.46E-02	2.21E-03	-2.23E-04	6.66E-06	7.49E-03
Pu-241	-1.10E-02	9.18E-02	1.38E-01	-2.58E-05	-6.85E-05	1.42E-05	2.29E-01
Pu-242	-1.23E-02	3.91E-03	5.66E-03	1.80E-04	-8.35E-05	5.08E-06	-2.63E-03
Total	-4.29E-01	6.57E-01	1.00E+00	1.72E-02	-8.91E-03	8.30E-04	1.24E+00

The sensitivity coefficients of U-238 in the 3D heterogeneous and RZ homogeneous calculation models are shown in Figure 2 for the sake of comparison. The sensitivity due to neutron capture reaction dominates in the RZ model. However, in the 3D heterogeneous model, the contribution of the neutron capture reaction decreases and the sensitivities of the fission and $\overline{\nu}$ in the upper energy region (above 1 MeV) increases. The sensitivity of the inelastic scattering reaction also increased in the 3D heterogeneous calculation model. This is due to the spectrum is harder than in the RZ model.

Figure 2: Sensitivity coefficients for U-238

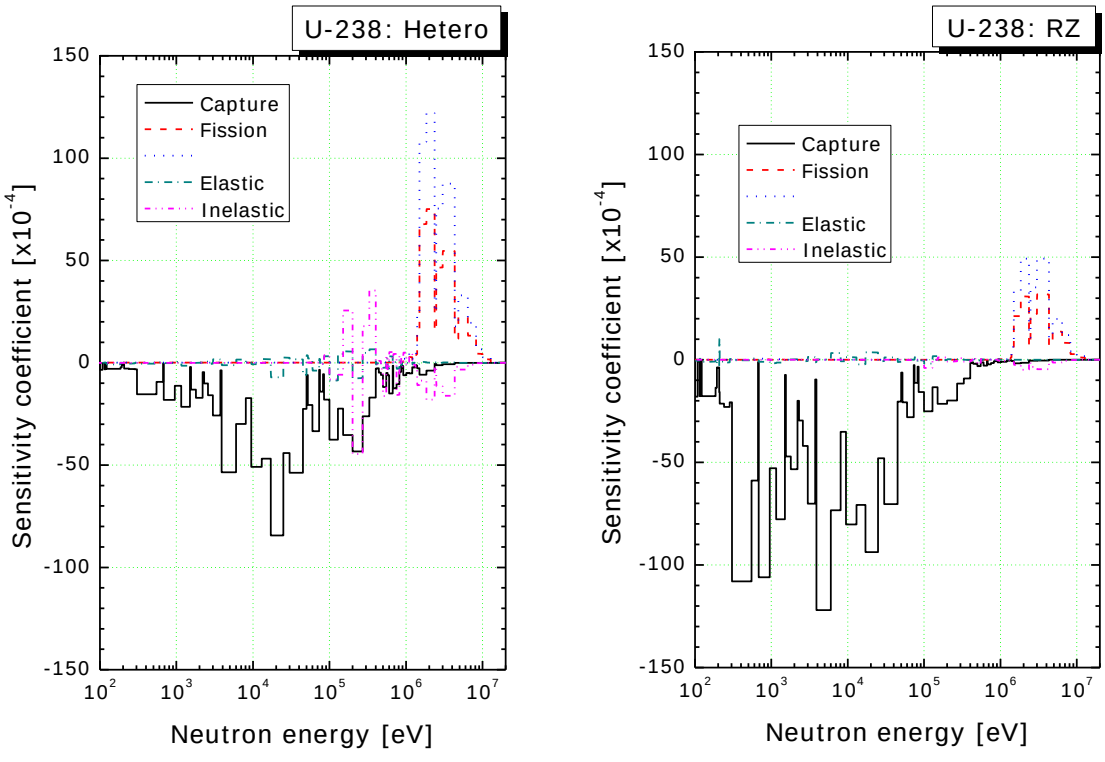

Uncertainty analysis

The uncertainty analysis was performed using the sensitivity coefficients shown in Table 1 and Table 2. Three calculation cases were prepared. The first case employed the SCALE 44-group covariance data and the sensitivity coefficients calculated in the 3D heterogeneous calculation model. The SCALE 44-group covariance data are constructed on the basis of covariance data from various libraries, including ENDF/B-VII, ENDF/B-VI, JENDL-3.3 and approximate uncertainties [13]. The second case dealt with the covariance data from TENDL-2009 library [15]. In the third case the SCALE 44-group covariance data and the sensitivity coefficients calculated in the RZ calculation model were used.

SCALE 44-group covariance data contain all data for all nuclides and reactions of interest listed in Table 1 and Table 2, while TENDl-2009 lacks χ (fission spectrum covariance) and $\overline{\nu}$. Enhancement of correlation between other reactions such as Capture-Fission is the feature of TENDL-2009 covariance data.

Table 3 shows the uncertainties deduced from covariance data with 1σ confidence. The uncertainty in the 3D heterogeneous model is slightly smaller than uncertainty in the RZ model. The main reason of this difference could be attributed to a decrease of the sensitivity coefficients for the neutron capture reaction in the 3D heterogeneous model. On the other hand, the SCALE-6 / TENDL-2009 result is about twice larger than other uncertainties. Thus the uncertainty for the same calculation model and tool strongly depends on covariance data used.

Table 3: Uncertainty deduced from covariance data

Model	Covariance data	Uncertainty (%)
3D heterogeneous	SCALE-6 44-group	0.94
3D heterogeneous	TENDL-2009	1.9
RZ homogeneous	SCALE-6 44 group	1.0

The contributions of each nuclide and reaction to the uncertainty are plotted on Figure 3. The contribution of neutron capture reaction in the 3D heterogeneous model is smaller than in case of the RZ model, especially for fuel nuclides (U and Pu). On the other hand, due to hardness of the spectrum, the contributions of neutron induced fission and $\overline{\nu}$ increases in 3D model, especially for Pu-238, Pu-240 and Pu-242. It is seen from the Figure 3 that the effect of inelastic scattering for U-238 is large in 3D model.

Figure 3: Uncertainties deduced from covariance data

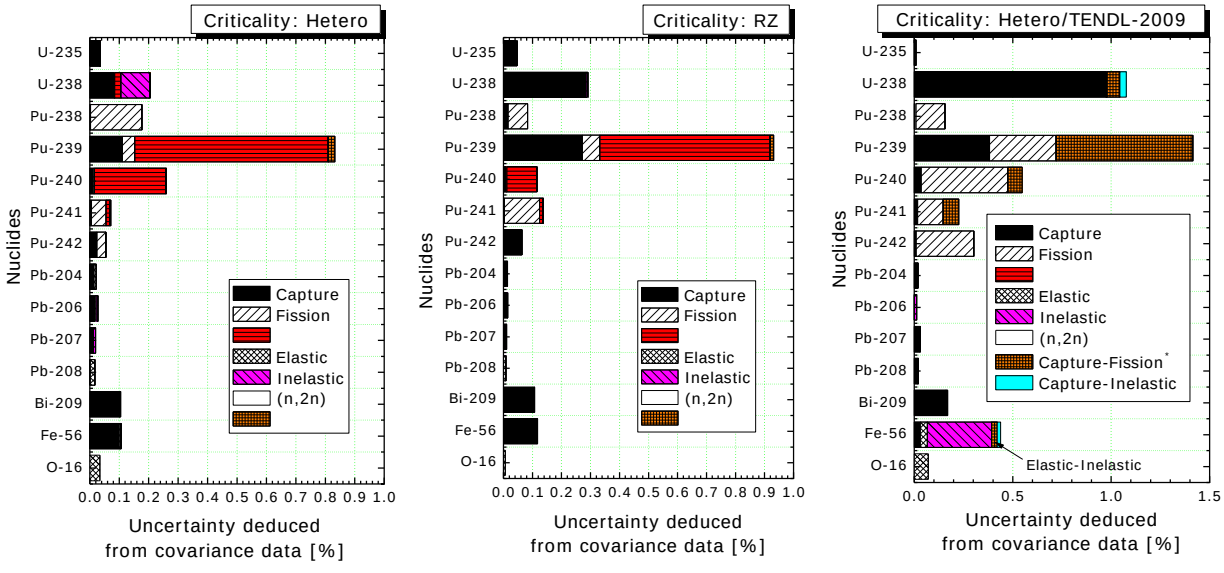

Significant differences are observed when comparing SCALE-6 44-group and TENDL-2009 covariance data. For example, the neutron capture reaction dominates for U-238 with the covariance data from TENDL-2009, while the contribution of capture reaction in the SCALE-6 44-group case is not so large. There are substantial differences for Pu isotopes and Fe-56. The contribution of correlations between other reactions is not negligible as it could be seen from TENDL-2009 case.

Comparison with MCNPX results

The MCNPX calculation of k_{eff} was performed for detailed 3D heterogeneous model. Although the discussion on uncertainty should normally be related to experimental data, there are no integral experimental data for a LBE-cooled core with MOX fuel. Thus MCNPX calculation results play role of experimental data in this case.

The results of SCALE-6 and MCNPX calculations with 3D model are shown in Table 4. Three nuclear data libraries were used with MCNPX to estimate the influence of data library choice.

Table 4: Comparison of keff calculated by SCALE-6 and MCNPX

Code	Library	k_{eff}
SCALE-6	ENDF/B-VII.0	0.98305±0.00031
MCNPX	JEFF-3.1.1	0.98297±0.00027
MCNPX	JENDL-3.3	0.97578±0.00026
MCNPX	ENDF/B-VII.0	0.98046±0.00026

The use of JENDL-3.3 and ENDF/B-VII.0 with MCNPX results in 0.73% and 0.26% lower k_{eff} value than JEFF-3.1.1, accordingly. It is however less than uncertainty margins shown in Table 3. This means that uncertainty deduced from covariance data covers the differences in k_{eff} due to data library variation in MCNPX calculation.

To investigate the "weight" of each nuclide in keff calculated with MCNPX, the variation of data library was employed for each particular nuclide. JEFF-3.1.1 library always served as reference. The black open rectangles on Figure 4 correspond to the use of JENDL-3.3 for each particular nuclide while JEFF-3.1.1 was used for other nuclides shown on the plot. The red open circles denote the use of ENDF/B-VII.0. Uncertainties deduced from covariance data from Figure 3 (obtained with SCALE-6 44-group calculation, left-hand plot) are shown for the sake of comparison. It is seen from Figure 4 that uncertainties deduced from covariance data do not cover the difference caused by data library variation in MCNPX calculation for U-235, Pu-240, Pb-207, Pb-208, Bi-209 and O-16. This may indicate that covariance data are underestimated.

As it is seen in Figure 3, the uncertainties deduced from the covariance data varied significantly with the change of covariance data. Although the uncertainties deduced from the covariance data ensured the differences in the MCNPX calculation, the contribution of each nuclide and reaction was different in each covariance data set. These results indicate that the covariance data of the nuclear data libraries is an open issue to discuss the reliability of the neutronics design.

The target accuracy for the fast reactor nuclear design is discussed in [16] where 0.3%Δk (1σ confidence) was proposed as limiting value for k_{eff} uncertainty. The uncertainties deduced from the covariance data for XT-ADS do not meet this criterion. The uncertainties will obviously be reduced by performing the integral experiments in LBE or Pb moderated environment with MOX or Uranium fuel. The reduction of uncertainties of U-238 neutron capture and inelastic scattering, Pu-238 fission, Pu-239 neutron capture and $\overline{\nu}$, Pu-240 $\overline{\nu}$, Bi-209 and Fe-56 neutron capture is required.

Figure 4: Uncertainties deduced from covariance data by SCALE-6 44-group and difference in MCNPX calculation by data library variation

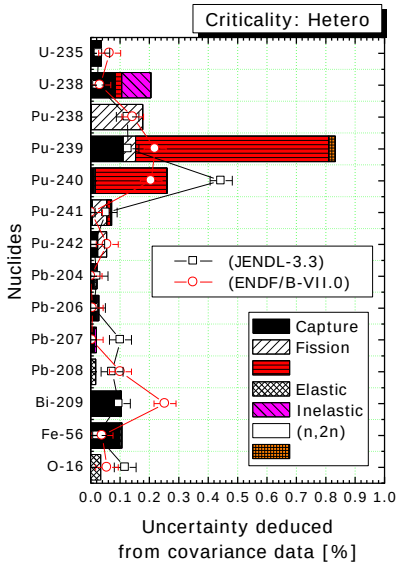

Conclusions

The sensitivity and uncertainty analysis was performed to confirm the reliability of the calculated effective neutron multiplication factor for the XT-ADS neutronics model.

The obtained sensitivity coefficients differ substantially between the 3D heterogeneous and RZ homogenized calculation models. The uncertainties deduced from the covariance data strongly depend on the covariance data variation. The covariance data of the nuclear data libraries is an open issue to discuss the reliability of the neutronics design. The uncertainties deduced from the covariance data for XT-ADS are 0.94% and1.9% by the SCALE-6 44-group and TENDL-2009 covariance data, accordingly. The uncertainties exceed the 0.3%Δk (confidence level 1σ) target accuracy level. To achieve this target accuracy, the uncertainties should be improved by experiments under adequate conditions such as LBE or Pb moderated environment with MOX or Uranium fuel.

References

[1] Aït Abderrahim, H., *et al.*, MYRRHA, a new future for nuclear research. DRAFT-2 pre-design File, *Report R-4234*, SCK·CEN (2006).

[2] De Bruyn, D., J.U. Knebel, "The Integrated Project EUROTRANS: EUROpean Research programme for the TRANSmutation of High Level Nuclear Waste in an Accelerator Driven System (ADS)", *Proc. of the 38th Annual Meeting of the IAEA Technical Working Group on Fast reactors & Accelerator Driven Systems*, Sao Paolo & Rio de Janeiro, Brazil (2005).

[3] Salvatores, M., *et al.,* "Needs and Issues of Covariance Data Application", *Nuclear Data Sheets*, 109, 2725–2732 (2008).

[4] Palmiotti, G., *et al.,* "A Global Approach to the Physics Validation of Simulation Codes for Future Nuclear Systems", *Proc. of the International Conference on Reactor Physics, Nuclear Power: A Sustainable Resource (PHYSOR'08)*, Interlaken, Switzerland (2008).

[5] Rearden, B.T., D.E. Mueller, "Recent Use of Covariance Data for Criticality Safety Assessment", *Nuclear Data Sheets*, 109, 2739–2744 (2008).

[6] Sugawara, T., T. Sasa, H. Oigawa, "Improvement Effect of Neutronics Design Accuracy by Conducting MA-loaded Critical Experiments in J-PARC", *Proc. of International Conference on Reactor Physics, Nuclear Power: A Sustainable Resource (PHYSOR'08)*, Interlaken, Switzerland (2008).

[7] Sugawara, T., *et al.,* "Analytical Validation of Uncertainty in Reactor Physics Parameters for Nuclear Transmutation Systems", *Journal of Nuclear Science and Technology*, 47, (6), 521-530 (2010).

[8] Shibata, K., *et al.,* "Japanese evaluated nuclear data library version 3 revision-3; JENDL-3.3", *Journal of Nuclear Science and Technology*, 39, (11), 1125–1136 (2002).

[9] Pelowitz, D.B., Ed., MCNPX User's Manual, Version 2.6.0, LA-CP-07-1473 (2008), and Pelowitz, D.B., *et al.,* MCNPX 2.7.C Extensions, LA-UR-10-00481, Los Alamos National Laboratory (2010).

[10] Artioli, C., *et al.,* "Minor actinide transmutation in ADS: the EFIT core design", *Proc. of International Conference on Reactor Physics, Nuclear Power: A Sustainable Resource (PHYSOR'08),* Interlaken, Switzerland (2008).

[11] Van den Eynde, G., *et al.*, "Neutronic design of the XT-ADS core", *Proc. of International Conference on Reactor Physics, Nuclear Power: A Sustainable Resource (PHYSOR'08),* Interlaken, Switzerland (2008).

[12] Sugawara, T., *et al.*, "Nuclear data sensitivity and uncertainty for XT-ADS", submitted to Annals of Nuclear Energy (2010).

[13] ORNL, SCALE: A Modular Code System for Performing Standardized Computer Analyses for Licensing Evaluation. ORNL/TM-2005/39 Version 6 Vols. I-III, Oak Ridge National Laboratory (2009).

[14] Chadwick, M.B., *et al.,* "ENDF/B-VII.0: Next Generation Evaluated Nuclear Data Library for Nuclear Science and Technology", *Nuclear Data Sheets*, 107, (12), 2931–3060 (2006).

[15] Koning, A., D. Rochman, TENDL-2009: TALYS-based Evaluated Nuclear Data Library including covariance data, JEFF/DOC-1310, OECD/NEA (2009).

[16] Ishikawa, M., "Application of covariances to fast reactor core analysis", *Nuclear Data Sheets*, 109, 2778-2784 (2008).

Where are the data? – Status report on the work with a new compilation of experimental nuclear total reaction cross-section data

Mattias Lantz[1,2], **Lembit Sihver**[3,4,5]
[1]Applied Nuclear Physics, Department of Physics and Astronomy,
Uppsala University, Uppsala, Sweden
[2]RIKEN Nishina Center, RIKEN, Wako, Saitama, Japan
[3]Nuclear Engineering, Applied Physics, Chalmers University of Technology,
Göteborg, Sweden
[4]Roanoke College, Salem, Virginia, USA
[5]Texas A&M University, TAMU-3133, College Station, Texas, USA

Abstract

The nucleon-nucleus and nucleus-nucleus total reaction cross-sections are of importance in many different fields, both for a better theoretical understanding as well as for a number of applications. The total reaction cross-section determines the mean free path when particles traverse nuclear matter, and the production cross-sections for secondary particles are directly proportional to it. Many complex Monte Carlo codes use the total reaction cross-sections for these purposes, and these observables become important in a number of different applications, including Accelerator Driven Systems, space radiation dosimetry, ion beam cancer treatment, and Single Event Effects (SEE) in digital electronics.

We have performed a comprehensive literature study in order to find all available experimental data on total reaction cross-sections, interaction cross-sections, and total charge changing cross-sections for neutrons, protons, and all stable and exotic heavy ions. The database extends earlier compilations with new data and data that have not been found in earlier searches. Excluded from the database are measurements where the cross-sections have been derived through model-dependent calculations from other kinds of measurements. The objective of the study is to identify where more measurements are needed in view of different applications, and to make the data easily available for model developers and experimentalists, as well as for the nuclear databases such as EXFOR. We will present some examples from the study, which is in the stage of quality control of all the gathered data.

Introduction

Total reaction cross-sections determine the probability that a nuclear particle undergoes a non-elastic interaction when passing through nuclear matter. Besides providing an additional constraint in the analyses of angular distributions for elastic scattering, it determines the mean-free path for the interaction length. Thus it is of importance for a number of applications where nucleons or nuclei traverse nuclear matter, including nuclear power technology. In complex Monte Carlo particle and heavy ion transport codes, such as FLUKA [1,2], GEANT [3,4] and PHITS [5], the total reaction cross-section is used for the determination of where the first interaction will occur when a particle traverses nuclear matter. In some cases it is also used as scaling factor for individual reactions, *i.e.* the cross-sections for each individual reaction channel follows the energy dependence of the total reaction cross-section. This paper is a status report on the work with a new compilation of experimental data for total reaction cross-sections, and related observables, for neutrons, protons and heavy ions. In the present paper we report on the motivation for, and the status of, the compilation work. Some of the challenges with the compilation, and our selected philosophy for which data that will be included, will be discussed.

Definitions

When a nuclear particle is incident on an atomic nucleus there are three different possibilities for what kind of interaction that will occur:

(1): The particle passes by the nucleus without any kind of interaction.

(2): The particle undergoes elastic scattering with the target nucleus. Both the incident particle and the target nucleus remain in their ground states and the only transfer of energy is due to the kinematics of the elastic interaction. The total elastic cross-section, denoted σ_{El}, is many times determined from the integrated differential cross-sections for elastic scattering.

(3): The particle undergoes some kind of non-elastic interaction, *i.e.* a reaction, with the target nucleus. The sum of the cross-sections for all possible reactions is the total reaction cross-section, denoted σ_R.

The total reaction cross-section, the interaction cross-section σ_I, and the total charge changing cross-section σ_{CC}, are defined as,

$$\sigma_{Tot} = \sigma_R + \sigma_{El}, \quad (1)$$

$$\sigma_I = \sigma_R - \sigma_{inel}, \quad (2)$$

$$\sigma_{CC} = \sigma(\Delta Z \geq 1), \quad (3)$$

where σ_{Tot}, is the total cross-section, σ_{inel} is the inelastic cross-section, and ΔZ is the change in atomic number. The interaction cross-section, follows the definition given by Kohama *et al.* [6], and includes all reaction channels that cause a change in the number of nucleons in the projectile. The cross-section for inelastic channels, σ_{inel}, includes all channels where the incident nucleus is excited without changing the number of nucleons, with or without any excitation or breakup of the target nucleus. The interaction cross-sections have mainly been measured for neutron-rich nuclei, and are convenient observables for studies of short-lived exotic nuclei. The values tend to be 80-90% of the total reaction cross-section, but at higher energies the two observables become more similar. A third related observable is the charge changing cross-section, σ_{CC}, which is defined as the cross-section for the projectile to change its number of protons. The energy behaviour is very similar to the interaction cross-section, *i.e.* with values that are 80-90% of the total reaction cross-section at energies below 1 GeV per nucleon.

The available experimental data on total reaction cross-sections for the projectiles proton, neutron and ^{12}C on carbon targets are shown in Figure 1. The energy dependence is similar for the three projectiles. In general, the shapes of the energy dependencies follow the nucleon-nucleon total cross-sections, with a decrease from low energies down to a dip at about 200-300 MeV/nucleon, and thereafter a slight increase due to the new reaction channels that open, *i.e.* pion production. For charged ions there is also the Coulomb barrier that brings the cross-section to zero at low energies. Neutrons do not have this barrier, though the available experimental data for the example in the figure seem to indicate such behaviour.

Figure 1: The available experimental data clearly shows the similarity in energy dependence on total reaction cross-sections for p+C (black dots), n+C (red circles) and 12C+C (blue triangles)

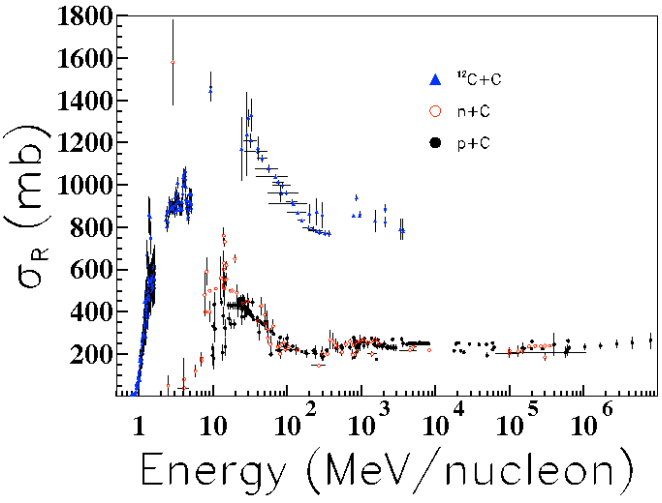

Motivation

There are already a number of compilations of total reaction cross-section data available, so why make another one? For protons the Bauhoff compilation [7] included experimental data up to 1 GeV. It was later updated and corrected by Carlson [8]. In parallel, Barashenkov compiled data for protons and other particles over a wide energy range [9,10]. The authors do not seem to have been aware of each other's work, because there is no complete overlap in any direction. Furthermore, the Barashenkov compilation includes data that have been derived from other particles. For instance there are data for neutrons that have been derived from proton measurements, and are thus not from real measurements with neutron beams. We have also observed that in many articles the authors seem to prefer data from the Bauhoff compilation instead of the later version by Carlson. After some investigation, including interrogation of a few authors, the reason was found to be that the Bauhoff compilation seems to include more target isotopes than the updated version by Carlson. This, however, is an unfortunate misunderstanding, because Carlson has corrected the isotopes for all measurements to the actual composition instead of what is written in the title of each article (it is quite common that it differs). And there are good reasons to trust the corrections by Carlson, since the majority of the data in the Bauhoff compilation comes from experiments performed by Carlson and co-workers. Furthermore, the 230 extra data points should make the Carlson compilation more attractive than the earlier version.

The EXFOR database, which is provided by the international network of nuclear data centres [11-14], is an important source for anyone who needs to obtain experimental data. We want to emphasize the importance that all experimentalists report their published nuclear measurements to this database. Although it may be somewhat difficult to use, this should be the primary source for anyone who wants to obtain nuclear data.

For heavy ions there are several authors that have made extensive comparisons of experimental data with their own measurements or calculations, thus producing articles with valuable collections of data. However, none of these collections is complete in any sense, and they are scattered in various publications. There are also a large number of published experimental data that seems to have been forgotten. Therefore we have initiated the effort of gathering all available data in one place in order to make it easily available for experimentalists and model makers. It is our ambition to find most of the data ever published until the year 2010.

A few challenges, how to scrutinize the data?

At present the work with the compilation is approaching the end of the collection phase, and the quality control phase will be started. When it comes to the quality control, it is important to emphasize that in order to not introduce further bias we will scrutinize the experimental data with respect to the experimental method being used, not with respect to the experimental result. In other words, we will accept data that seem to disagree significantly with the general trends as long as the experimental method is acceptable, while we may ignore seemingly high quality data that are based on questionable methods. In order to find out about the experimental methods it is often necessary to consult related articles or technical reports that are not published.

A priority list for different kinds of experimental methods will be set up, and data based on methods that do not fulfil the requirements will be omitted, alternatively be properly flagged. It should be noted that almost all experimental methods depend on some theoretical stage for certain kinds of corrections. Our purpose is to discriminate methods where the final result depends more on a theoretical model than on the experiment itself. One clear case is total reaction cross-sections derived with optical model calculations fitted to experimental differential cross-sections of elastic scattering. Although the differential cross-sections may be measured with high quality, the derived total reaction cross-section will depend significantly on the parameters used in the optical model.

Other aspects that need to be considered are how to handle data that are only available in conference proceedings or technical reports, but never have been published in a peer-review journal. There could be good reasons why the data never reached a wider distribution, and therefore one could easily decide to not include any data from such reports. On the other hand, in several countries and laboratories there has until recently not existed any incentive to publish experimental results, and therefore these data could very well be of high quality. With these opposite views in mind, our selected strategy is to scrutinize the technical reports in the same way as for peer-reviewed journal articles, *i.e.* by examining the experimental method. Accepted data that has not been peer-reviewed will be flagged accordingly.

Present status

In Figure 2 the upper left panel shows the available experimental data where protons are the projectile. The blue dots are the data given in the Barashenkov compilation [10], and the black dots are the data given in the Carlson compilation [8]. There are not so many black dots seen, the reason being that they are already included in the Barashenkov compilation, and therefore covered by blue dots. The red dots are the data given in the present work that were not included in any of the earlier compilations. As seen there are quite a lot of data available for protons, and there are also plenty of data for neutrons. The situation is much worse for other projectiles, although dedicated programs for measurements of heavy ions are in progress [15]. The upper right panel shows the situation where carbon isotopes are either projectile or target, and the lower panel shows the same situation for iron isotopes. Not surprisingly, the amount of experimental data tends to decrease with projectile mass, mainly due to experimental difficulties.

At present (October 2010) we have data from about 600 different articles, conference proceedings and technical reports, covering the following systems:

- σ_R for
  - p+A (2100 data points)
  - n+A (1100 data points)
  - A+A (2900 data points)
- σ_I for A+A (400 data points)
- σ_{CC} for A+A (900 data points)
- σ_{Tot} for p+A, A+A (300 data points)

Data for σ_{Tot} for n+A are not included since they are well covered in other databases. The total number of data points is subject to change, depending on where we will set the threshold level in

Figure 2: Upper left: The available experimental data for protons on different targets, plotted as function of element Z, and at all energies. Blue dots are from the Barashenkov compilation [10], black dots from the Carlson compilation [8], and red dots are the "new" data that have been found in the present work. Upper right shows the available experimental data where carbon isotopes are either the projectile (blue dots), target (black dots), or both (red dot). In a similar manner the lower left shows the situation for iron isotopes, with red dots for iron as projectile and blue circles for iron as target.

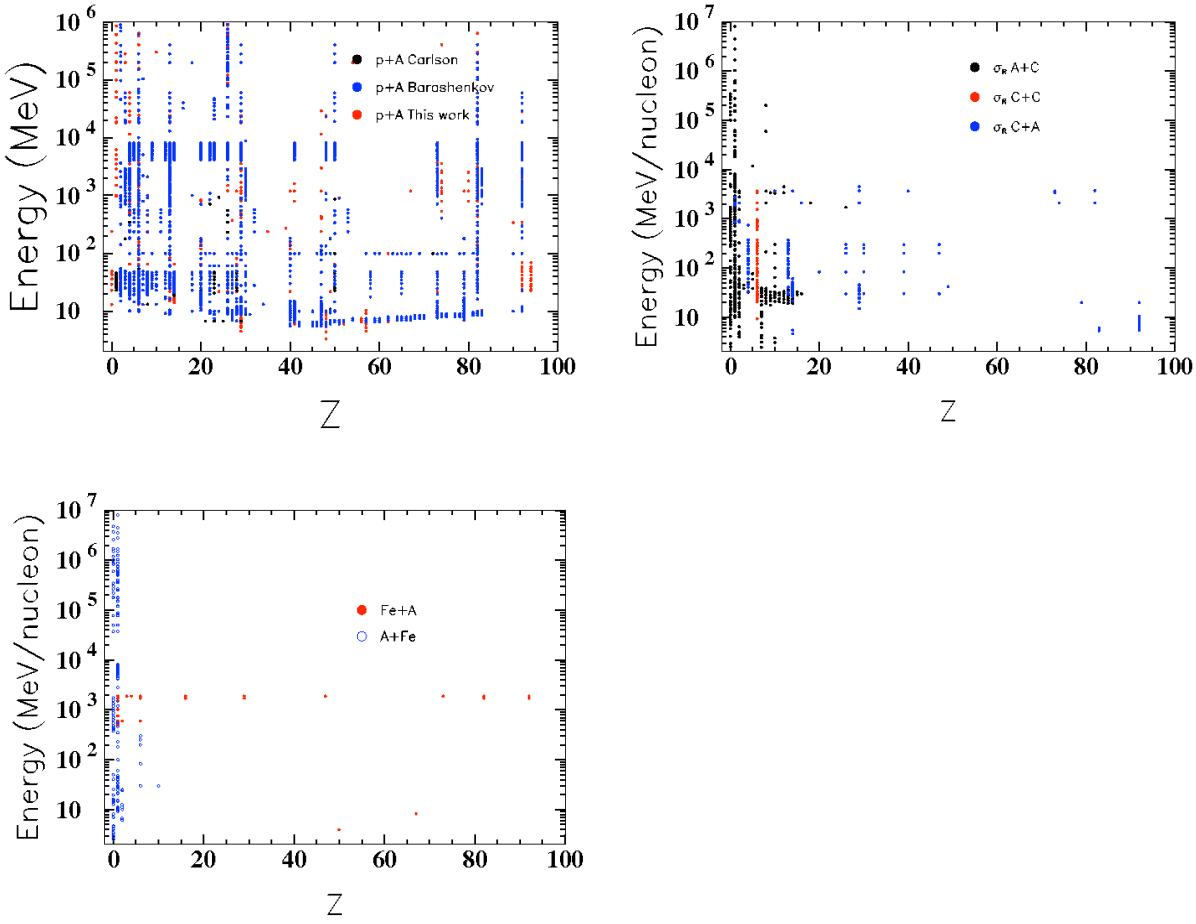

the quality control. There may also be additional data included from some of the reports that we are still trying to obtain. Figure 3 shows the present look of a typical data table in the compilation. There may be more columns added depending on what kind of information that potential users of the database would like to see included. We would appreciate such kind of feedback from the nuclear data community in order to improve the quality and usefulness of the compilation.

Benefits of the work

The motivation for performing this work is mainly to use the data in model inter-comparisons and development, and to obtain an overview of what data that needs to be measured in order to improve the models. For instance, a dedicated program for systematic model inter-comparisons has been initiated, starting with nuclei of relevance for space radiation protection and dosimetry [16]. We are also using the database in order to plan for measurements, and to suggest measurements by other groups.

Figure 3: The present look of the compilation. There is an attempt to separate statistical and systematic errors, wherever the relevant information is given. The laboratory or institute where the data were measured are given with same coding as in the EXFOR database. Data that are already given in the EXFOR database are denoted with the corresponding entry code.

Proj	Target	Energy MeV/A	ΔE MeV/A	σ_R mb	$\Delta^{stat}\sigma_R$ mb	$\Delta^{syst}\sigma_R$ mb	Laboratory	Exp. method	Notes	EXFOR Entry	Ref
^{2}H	Fe	6.7		1577	68	15	4UKRIJD	Tra,FC		F0579.003	[209]
^{2}H	Fe	11.2		1370	70		1USABRK	Tra			[558]
^{2}H	Fe	12.55	0.2	1676	49		3ARGCNE	Tra		D0223.008	[380]
^{2}H	^{58}Co	6.7		1609	41	17	4UKRIJD	Tra,FC		F0579.004	[209]
^{2}H	Co	12.6	0.2	1586	49		3ARGCNE	Tra		D0223.010	[380]
^{2}H	Ni	5.515	0.235	1460	60		2UK HAR	Tra		D0314.016	[85, 86]
^{2}H	Ni	5.75	0.225	1460	60		2UK HAR	Tra		D0314.016	[85, 86]
^{2}H	Ni	6.6		1457	33		4UKRIJD	Tra,FC		F0579.005	[209]
^{2}H	Ni	11.2		1491	63		1USABRK	Tra			[558]
^{2}H	Ni	12.55	0.2	1537	48		3ARGCNE	Tra		D0223.009	[380]
^{2}H	^{58}Ni	5.49	0.26	1375	61		2UK HAR	Tra		D0314.017	[85]
^{2}H	^{58}Ni	6.4		1589	125		3POLIFJ			D0576.003	[133, 134]
^{2}H	^{58}Ni	18.95	0.10	1625	51	33	2SWDUPP	Tra		A0604.008	[59]
^{2}H	^{58}Ni	32.75	0.25	1571	33	31	2SWDUPP	Tra		A0604.008	[59]
^{2}H	^{58}Ni	48.7	0.15	1524	45	30	2SWDUPP	Tra		A0604.008	[59]
^{2}H	^{60}Ni	5.03	0.22	1441	60		2UK HAR	Tra		D0314.018	[85]
^{2}H	^{60}Ni	5.55	0.20	1508	63		2UK HAR	Tra		D0314.018	[85]
^{2}H	^{60}Ni	6.4		1523	120		3POLIFJ			D0576.008	[133, 134]
^{2}H	^{60}Ni	6.8		1536	125		4UKRIJD	Tra,FC		F0579.006	[209]
^{2}H	^{60}Ni	18.95	0.10	1698	49	33	2SWDUPP	Tra		A0604.009	[59]
^{2}H	^{60}Ni	32.75	0.25	1619	34	31	2SWDUPP	Tra		A0604.009	[59]
^{2}H	^{60}Ni	48.7	0.15	1588	40	30	2SWDUPP	Tra		A0604.009	[59]
^{2}H	^{61}Ni	6.73		1666	60		4UKRIJD	Tra,FC		F0579.007	[209]
^{2}H	Cu	5.505	0.245	1548	66		2UK HAR	Tra	x	D0314.019	[85]
^{2}H	Cu	11.2		1539	61		1USABRK	Tra			[558]

Outlook and conclusions

Once we have decided on a suitable threshold level for which experimental methods to include, and which that will be excluded, the data will be scrutinized according to the quality demands. Thereafter the database will be submitted for publication, in one or several articles, depending on how it should be divided. At that time it will also be made available for inclusion in the EXFOR database. Furthermore we are considering making data tables easily available in numerical form on a web site.

The work with a complete compilation of all available experimental data on total reaction cross-sections, and related observables, is motivated by the fact that there are plenty of data that seem to have been forgotten, mainly due to the huge task of finding the data. Furthermore, the available data compilations, and the EXFOR database, are incomplete and in some cases include inconsistencies. The compilation work is in the stage of quality control, although some more references are still to be obtained. Our objective is to publish the compilation as soon as possible, and at the same time make the data available for inclusion in the EXFOR database.

Acknowledgements

M. Lantz would like to acknowledge the financial support from the Japanese Society for the Promotion of Science (JSPS).

References

[1] Fassò, A., *et al.*, *FLUKA: a multi-particle transport code*, CERN-2005-10 (2005), INFN/TC_0511, SLAC-R-773.

[2] Battistoni, B., *et al.*, "The FLUKA code: Description and benchmarking", Proc. Hadronic Shower Simulation Workshop 2006, Fermilab, USA (2006).

[3] Sulkimo, J., *et al.*, "Geant4 – a simulation toolkit", *Nucl. Instrum. Meth.* A 506 (2003) 250-303.

[4] Allison, J., *et al.*, "Geant4 Developments and Applications", *IEEE Trans. Nucl. Sci.* 53, 270-278 (2006).

[5] Niita, K., *et al.*, "PHITS – a particle and heavy ion transport code system", *Radiat. Meas.* 41, 1080-1090 (2006).

[6] Kohama, A., K. Iida, K. Oyamatsu, "Difference between interaction cross-sections and reaction cross-sections", *Phys. Rev.* **C** 78, 061601(R) (2008).

[7] Bauhoff, W., "Tables of reaction and total cross-sections for proton-nucleus scattering below 1 GeV", *Atomic Data and Nuclear Data Tables* 35, 429-447 (1986).

[8] Carlson, R.F., "Proton-nucleus total reaction cross-sections and total cross-sections up to 1 GeV", *Atomic Data and Nuclear Data Tables* 63, 93-116 (1996).

[9] Barashenkov, V.S., "Interaction cross-sections of elementary particles", Jerusalem (1968).

[10] Barashenkov, V.S., "Cross-Sections of Interactions of Particle and Nuclei with Nuclei", JINR, Dubna, (in Russian) (1993).

[11] Brookhaven National Laboratory (BNL) – National Nuclear Data Center (NNDC), Experimental Nuclear Reaction Data (EXFOR / CSISRS), Brookhaven, Upton, NY., USA, url: *www.nndc.bnl.gov/exfor/exfor00.htm*.

[12] International Atomic Energy Agency (IAEA) – Nuclear Data Services, Experimental Nuclear Reaction Data (EXFOR), Vienna, Austria, url: *www-nds.iaea.org/exfor/exfor.htm*.

[13] OECD Nuclear Energy Agency (NEA) Data Bank – Nuclear Data Services, Paris, France, url: *www.oecd-nea.org/dbdata/x4/*.

[14] Russian Nuclear data Centre (CJD) – A.I. Liepunski Institute of Physics and Power Engineering (IPPE), Obninsk, Russia, url: *www.ippe.obninsk.ru/podr/cjd*.

[15] Takechi, M., *et al.*, "Reaction cross-sections at intermediate energies and Fermi-motion effect", *Phys. Rev.* C 79, 061601(R) (2009).

[16] Sihver, L., *et al.*, "A Comparison of Total Reaction Cross-Section Models used in Particle and Heavy Ion Transport Codes", *Proc. of the IEEE Aerospace Conf.*, Big Sky, MT, USA (2010).

Nuclear data needs for reactor graphite radiological characterization and recycling

A. Plukis, R. Plukienė, A. Puzas, V. Remeikis, G. Duškesas
Center for Physical Sciences and Technology, Vilnius, Lithuania

Abstract

Graphite is widely used material to moderate neutrons in nuclear reactors starting with Chicago Pile 1 in 1942. Management of irradiated graphite after end life of the reactor is an important task both to graphite moderated reactors in operation or decommissioning (Magnox, AGR, HTR, RBMK) and to new HTR reactors designs (generation IV reactors VHTR or MSR). The graphite recycling opportunity for re-use is technically challenging because of the high specifications of graphite required but also it is one of solution of irradiated graphite management instead of disposal. For graphite treatment, disposal or recycling concentration of radioactive contaminants in spent graphite should be identified.

Activity of radionuclides in irradiated graphite depends on concentration of impurities in virgin graphite and on characteristics of neutron flux. Concentrations of impurities in virgin graphite are usually unknown and have to be determined experimentally. As there are tens of important nuclides which have to be measured for modelling medium- and long-lived waste, it is not cost effective to measure all of them by expensive neutron activation analysis. Comparison of results on impurity concentration obtained with X-ray fluorescence technique, ICP-MS technique and neutron activation analysis for graphite irradiated in RBMK-1500 reactor has shown that precise enough determination of concentrations of elements Na, V, Zn, Ge, Ag, and Ta in graphite can be done only by neutron activation analysis.

Precise evaluation of the neutron fluence in different locations of the reactor graphite stack and other graphite constructions has been performed using Monte Carlo MCNPX code. The MCNPX calculation of the $^{13}C/^{12}C$ ratio in irradiated graphite has been validated against the $^{13}C/^{12}C$ ratio measured by stable isotope ratio mass spectrometry. For calculation of ^{14}C activity in graphite microscopic cross-sections of reactions $^{12}C(n, \gamma)^{13}C$, $^{13}C(n, \gamma)^{14}C$, and $^{14}N(n,p)^{14}C$ have been used. Analysis of data on these microscopic cross-sections in different databases has revealed their large uncertainty.

Introduction

Graphite is widely used material to moderate neutrons in nuclear reactors starting with Chicago Pile 1 in 1942. Management of irradiated graphite after end life of the reactor is an important task both to graphite moderated reactors in operation or decommissioning (Magnox, AGR, HTR, RBMK) and to new HTR reactors designs (generation IV reactors VHTR or MSR). The graphite recycling opportunity for re-use is technically challenging because of the high specifications of graphite required but also it is one of solution of irradiated graphite management instead of disposal. For graphite treatment, disposal or recycling concentration of radioactive contaminants in spent graphite should be identified.

Activity of radionuclides in irradiated graphite depends on concentration of impurities in virgin graphite and on characteristics of neutron flux. ^{14}C isotope is one of the limiting radionuclides for low- and intermediate-level radioactive waste of the RBMK-1500 reactor and graphite itself [1]. Miner concentrations (usually less than 0.01% [2,3]) of such impurities as Cs, Sr, Eu, Cd, U, Th after 20-30 years of irradiation by neutrons also results in radiological important activities of long-lived radionuclides [1,4].

Concentrations of impurities in virgin graphite are usually unknown and have to be determined experimentally. As there are tens of important nuclides which have to be measured for modelling medium- and long-lived waste, it is not cost effective to measure all of them by sensitive neutron activation analysis. In this work by comparison results obtained with X-ray fluorescence technique, ICP-MS technique and neutron activation analysis for graphite irradiated in RBMK-1500 reactor we have determined impurities for measurement of which use of neutron activation analysis is the preferable choice.

The other part of our work is devoted to show importance of some uncertainties of nuclear cross-sections for modelling of neutron activation in graphite moderated reactor. For this aim we applied Monte Carlo MCNPX code (v2.6 which includes CINDER burn-up capability) for calculation of activation of the graphite stack in the RBMK-1500 reactor.

Comparison of X-ray fluorescence, ICP-MS and neutron activation analysis results

The samples for measurement have been taken from the RBMK-1500 reactor fuel channel sleeve made of continuous graphite rings (for details see [5]).

For X-ray fluorescence measurement, 10 g of the sample was ground for 3 minutes with the mill made of stainless steel till homogeneous powder appeared. After that the sample powder was squeezed to the (3x1) cm cylinder shape tablet and placed into the X-ray spectrophotometer. X-ray fluorescence analysis has been carried out with the wavelength dispersive X-ray fluorescence spectrophotometer S4 Pioneer (Bruker).

For ICP-MS measurements a piece of graphite ring has been poured with 10 ml of 2 % nitric acid, closed with a parafilm tape and left for 72 hours. After that 5 ml of solution were taken and diluted up to 15 ml with distilled water and ICP-MS measurements have been performed with the double focusing high resolution sector field inductively coupled plasma mass spectrometer Element 2 (Thermo Scientific).

For neutron activation analysis we refer to the older work [2] where the graphite specimens have been irradiated by the thermal and fast neutron flux in the CEA research reactors ORPHEE and OSIRIS (Φ_{th} = (1.2–2.5) × 10^{13} n (cm^{-2} s–1) for ORPHEE and Φ_{fast} = 2 × 10^{13} n (cm^{-2} s^{-1}) for OSIRIS). After irradiation the specimens have been processed and analyzed by gamma spectrometry.

Results on the concentrations of elements in RBMK-1500 reactor fuel channel sleeve and relative standard deviations (RSD) are provided in Table 1.

As seen from Table 1 precise enough determination of concentrations of elements Na, V, Zn, Ge, Ag, and Ta in graphite can be done only by neutron activation analysis.

Table 1: Comparison of X-ray fluorescence and ICP-MS results with neutron activation analysis

	X-Ray Fluorescence		ICP-MS		Neutron activation [2]	
Element	Concentr., g/g	RSD (%)	Concentr., g/g	RSD (%)	Concentr., g/g	RSD (%)
Na	-	-	3.61E-05	4.2	4.6E-06	6.3
Mg	-	-	2.78E-06	12.5	7.0E-06	-
Al	2.00E-04	10.7	1.12E-05	2.9	9.2E-06	1.3
Cl	-	-	1.55E-05	7.9	7.6E-06	2.3
K	2.00E-05	9.4	2.21E-05	2.0	1.9E-06	12.0
Ca	2.55E-04	1.8	7.50E-05	4.1	5.2E-05	4.3
Ti	-	-	3.80E-06	3.9	1.7E-05	2.7
V	-	-	1.90E-07	4.0	1.7E-05	1.3
Cr	-	-	4.68E-07	5.5	6.0E-07	1.7
Mn	-	-	5.93E-07	3.4	5.8E-07	1.7
Fe	4.00E-05	2.8	4.07E-05	4.1	1.9E-05	5.3
Co	-	-	3.52E-08	11.3	1.9E-08	0.7
Ni	-	-	6.13E-07	4.4	3.9E-07	8.3
Zn	-	-	2.72E-06	3.6	2.0E-08	-
Ga	-	-	4.29E-09	37.8	1.0E-08	-
Ge	-	-	2.10E-09	200.2	9.0E-06	-
Sr	-	-	1.06E-06	5.8	9.6E-07	5.7
Zr	-	-	7.27E-07	7.4	1.0E-06	7.0
Mo	-	-	5.81E-08	26.6	1.7E-07	0.7
Ag	-	-	6.53E-08	14.1	3.0E-09	20.0
Cs	-	-	2.11E-09	33.6	1.6E-09	9.3
Ba	-	-	1.29E-06	1.4	2.0E-06	2.3
Eu	-	-	2.34E-09	50.0	2.6E-09	2.0
Ho	-	-	2.08E-09	38.1	9.4E-09	6.7
Hf	-	-	1.47E-08	24.4	5.8E-09	1.7
Ta	-	-	2.39E-10	104.2	1.9E-09	3.3
W	-	-	4.20E-08	11.8	4.7E-08	3.7
Th	-	-	3.37E-09	26.4	7.9E-09	1.7
U	-	-	5.35E-09	18.8	1.6E-08	2.7

Importance of cross-sections of carbon isotopes for evaluation of the neutron fluence in the graphite

A method to restore the irradiation parameters of graphite or other carbonaceous materials by using experimental and modelling results of ^{13}C generation in the irradiated material is developed in [6]. It is based on comparison of results of stable isotope ratio mass spectrometry for the ratio of concentrations $^{13}C/^{12}C$ in virgin and irradiated carbonaceous material with results of computer simulation of neutron activation for the ratio of concentrations $^{13}C/^{12}C$ in irradiated carbonaceous material.

Ability of the method to evaluate the realistic characteristics of the reactor core such as the neutron fluence in any position of the reactor graphite stack or other graphite constructions has

been demonstrated by comparison of simulated activity of ^{14}C with the one measured by the β spectrometry technique for RBMK-1500 reactor of Ignalina NPP. For this purpose the ^{13}C and ^{14}C content of irradiated graphite of the RBMK-1500 reactor has been evaluated by employing the Monte Carlo N-Particle Code (MCNPX) computer code version 2.6 [6] which includes the CINDER90 [7, 8] code for calculation of activation using a simplified 3D model with periodical boundary conditions (see horizontal section of the model in Figure 1, where red circles represent UO_2 fuel with Zr + 1 wt.%Nb cladding, green ring - fuel channel tube from Zr + 2.5 wt.%Nb, bluish area inside green ring - coolant water, blue ring - graphite sleeve and blue area outside blue ring - graphite stack).

Figure 1: Horizontal section of 3D model of the reactor fuel assembly in the graphite matrix

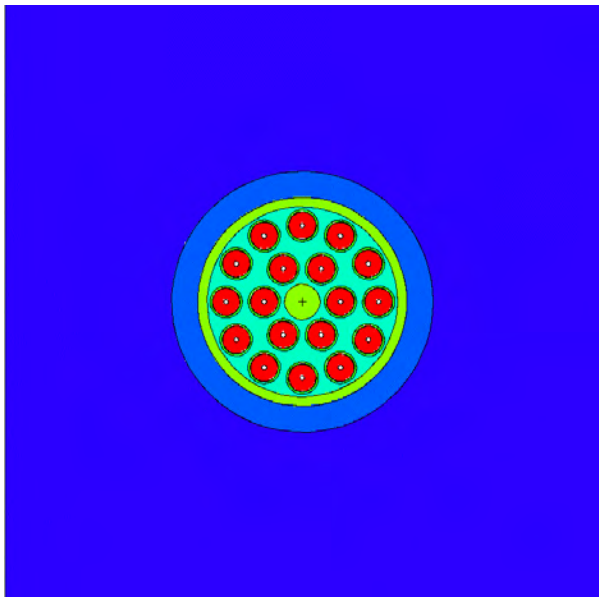

As the first step of calculation, the neutron flux in the RBMK-1500 reactor graphite has been obtained by the MCNPX code (details of input are provided in [5]). An evolution of the fuel isotopic composition, activation and radioactive decay of nuclei during irradiation has been simulated with the CINDER90 code which is incorporated in MCNPX. The CINDER90 code uses 63 neutron energy groups and has its own nuclear data library composed mainly of ENDF, JEF and JENDL [7] data libraries as well as other data (*e.g.* for $^{13}C(n, \gamma)^{14}C$ reaction ACTL neutron activation cross-section library [9] is used). The main reason why CINDER90 data library has been chosen in our work is the presence of the microscopic cross-sections for $^{12}C(n, \gamma)^{13}C$ reaction in this library. These microscopic cross-sections are absent in other nuclear data libraries (for instance, in JEF-3.0, JENDL-3.3 and ENDF/B-VI) where only cross-section for natural C and no data for ^{12}C isotope are present).

In [6] MCNPX code has also been used to calculate the amount of ^{14}C generated in $^{14}N(n,p)^{14}C$ reaction in a similar way considering ENDF/B-VI microscopic cross-sections as in the case of $^{12}C(n, \gamma)^{13}C$, $^{13}C(n, \gamma)^{14}C$ reactions. Comparison of the newest ENDF/B-VII library nuclear data for $^{14}N(n,p)^{14}C$ reaction (which is the same as the ENDF/B-VI) with the cross-section of CINDER90 shows the 2 times difference. After comparison with other sources we have decided to make correction and to use the ENDFB-VI data library cross-sections for estimation of ^{14}N concentration. Microscopic cross-sections for $^{14}N(n,p)^{14}C$ reaction in different data libraries are provided in Figure 2.

Figure 2: Microscopic cross-sections for 14N(n,p)14C reaction in different data libraries

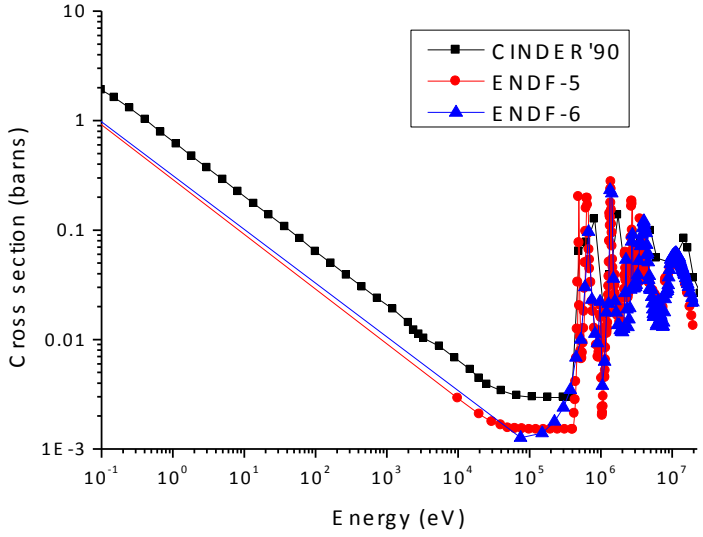

Conclusions

Although it is possible to use ICP-MS method for determination of concentrations of many elements in virgin graphite instead of neutron activation analysis but neutron activation analysis of impurities in graphite has to be done for determination of elemental concentrations of Na, V, Zn, Ge, Ag, and Ta.

For precise evaluation of the neutron fluence in any position of the graphite stack or other graphite constructions in the graphite moderated reactor and for determination of ^{14}C activity in carbonaceous materials uncertainties of microscopic cross-sections for reactions $^{12}C(n, \gamma)^{13}C$, $^{13}C(n, \gamma)^{14}C$, $^{13}C(n, \alpha)^{10}Be$, and $^{14}N(n,p)^{14}C$ have to be reduced.

Acknowledgements

The authors would like to acknowledge the financial support of European Commission (European Atomic Energy Community [EURATOM]) for funding project 211333 in the Seventh Framework programme.

The work has also been supported by Lithuanian Agency for Science, Innovation and Technology (contract No. 31V-180).

References

[1] Remeikis, V., *et al.* "Study of the nuclide inventory of operational radioactive waste for the RBMK-1500 reactor", Nucl. Eng. Des. 239, 813–818 (2009).

[2] Ancius, D., *et al*., "Evaluation of the activity of irradiated graphite in the Ignalina Nuclear Power Plant RBMK-1500 reactor", Nukleonika 50, 113-120 (2004).

[3] Bushuev, A.V., V.N. Zubarev, I.M. Proshin, "Composition and quantity of impurities in graphite of industrial reactors", At. Energ. 92, 331-335 (2002).

[4] Šmaižys, A., E. Narkūnas, P. Poškas, "Modeling of activation processes for GR-280 graphite at Ignalina NPP", Rad. Prot. Dosim. 116, 270-275 (2005).

[5] Remeikis, V., *et al*., "Method based on isotope ratio mass spectrometry for evaluation of carbon activation in the reactor graphite", Nucl. Eng. Des, 240, 2697-2703 (2010).

[6] Pelowitz, D.B., MCNPX User's Manual, Version 2.6.0, Report LA-CP-07-1473, Los Alamos National Laboratory, USA (2008).

[7] Wilson, W.B., *et al*., A Manual for CINDER'90 Version 07.4 Codes and Data, LA-UR-07-8412, Los Alamos National Laboratory, USA (2007).

[8] Fensin, M.L., J.S. Hendricks, S. Anghaie, "The Enhancements and Testing for the MCNPX 2.6.0 Depletion Capability", Nuc. Tech., 170(1), 68-79 (2010).

[9] Gardner, M.A., R.J. Howerton, ACTL - Evaluated Neutron Activation Cross-Section Library – Evaluation Techniques and Reaction Index, UCRL-50400, Vol. 18, Lawrence Livermore Laboratory, available from the Radiation Shielding Information Center, Oak Ridge under package name DLC-69/ACTL (1978).